SAND2022-7319C

# Base Pressure Fluctuation Modeling: Theory, Simulation and Measurement

Lawrence DeChant[1], Brian Robbins[2], Cory Stack[3], Ashley Saltzman[4]
*Sandia National Laboratories, Albuquerque, NM, 87185-0825*

**[Abstract]** The near wake flow field associated with hypersonic blunt bodies is characterized by complex physical phenomena resulting in both steady and time dependent pressure loadings on the base of the vehicle. Here, we focus on the unsteady fluid dynamic pressure fluctuation behavior as a vibratory input loading. Typically, these flows are characterized by a locally low-pressure, separated flow region with an unsteady formation of vortical cells that are locally produced and convected downstream into the far-field wake. This periodic production and transport of vortical elements is very-well known from classical incompressible fluid mechanics and is usually termed as the (Von) Karman vortex street. While traditionally discussed within the scope of incompressible flow, the periodic vortex shedding phenomenon is known for compressible flows as well. To support vehicle vibratory loading design computations, we examine a suite of analytical and high-fidelity computational models supported by dedicated experimental measurements. While large scale simulation approaches offer very high-quality results, they are impractical for design-level decisions, implying that analytically derived reduced order models are essential. The major portions of this effort include an examination of the DeChant-Smith Power Spectral Density (PSD) [1] model to better understand both overall Root Mean Square (RMS) magnitude and functional maximum associated with a critical vortex shedding phenomenon. The critical frequency is examined using computational, experiments and an analytical shear layer frequency model. Finally, the PSD magnitude maximum is studied using a theory-based approach connecting the PSD to the spatial correlation that strongly supports the DeChant-Smith PSD model behavior. These results combine to demonstrate that the current employed PSD models provide plausible reduced order closures for turbulent base pressure fluctuations for high Reynolds number flows over range of Mach numbers. Access to a reliable base pressure fluctuation model then permits simulation of bluff body vibratory input.

## Nomenclature

A = local constant
c = constant (locally defined)
c = a damping constant
$C_D$ = body drag coefficient
d,D = base diameter
f = frequency
h = vortex layer thickness
$M_e$ = edge Mach number
P = pressure
$q_e$ = edge dynamic pressure
$r_0$ = base diameter
Re = Reynolds number
$S_t$ = dimensionless vortex shedding frequency
S = dimensionless vortex shedding frquency
u = streamwise mean velocity
U = free stream
K = local constant
$K_C$ = Clauser constant =0.016
c = a damping constant estimated as 0.05 (additional development subsequently).
$q_e$ = edge dynamic pressure

[1,2,3,4] Technical Staff, Aerosciences Dept., P.O. 5800, MS 0825, Albuquerque, NM, 87185, Member AIAA

$\alpha,\beta$ = parameters
$\lambda$ = wavelength
$\omega$ = dimensionless angular frequency
$\theta$ = cone angle

Subscripts/superscripts

0 = constant
b = base
e = edge
mag = magnitude
rms = root mean square

# I. Introduction

Base pressure fluctuation and mean base pressure behavior is an important physical behavior associated with the near wake for blunt base geometries. Typically, these flows are characterized by a locally low-pressure, separated flow region with an unsteady formation of vortical cells that are locally produced and convected downstream into the far-field wake. This periodic production and transport of vortical elements is very-well known from classical incompressible fluid mechanics and is usually termed as the (von) Karman vortex street. While traditionally discussed within the scope of incompressible flow, the periodic vortex shedding phenomenon is known for compressible flows as well.

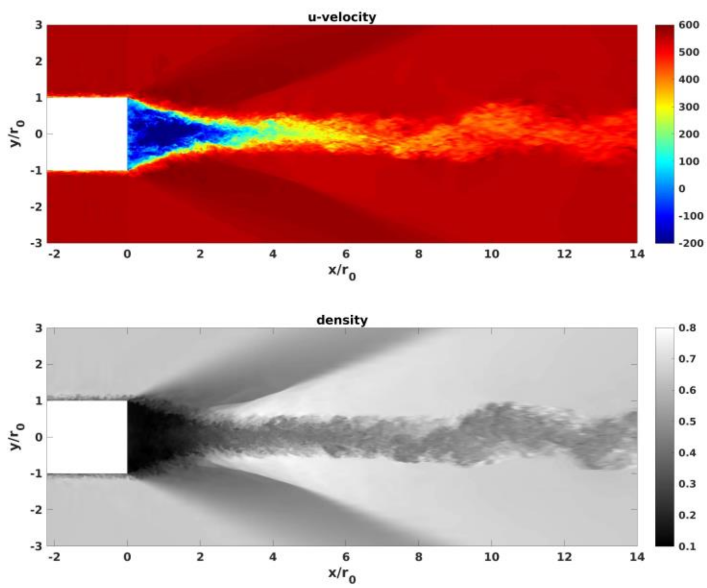


Figure 1. Base flow behavior for a bluff body using high fidelity LES simulations for a Mach 2.46 63.5 mm diameter after body

The unsteady periodic shedding behavior induces a flow-induced time dependent frequency. Coupling between the flow velocity field and the induced pressure through momentum conservation forms the basis for unsteady pressure loading associated with the bluff body base. Estimation of this loading is the focus of this discussion.

Base pressure fluctuation loading is typically describe using the frequency space auto-spectral density (ASD), or power spectral density (PSD), which inherently contains both spectral and magnitude information. DeChant and Smith [1] describe such a formulation where magnitude information and dominant frequency results are related to previous efforts such as Ahlborn [2] and Shvets [3]. The derivation of this model relies on an approximate unsteady vortex flow approach. This model has been successfully used for a wide range of loading simulation efforts where base pressure fluctuation effects play a relatively limited role. The overall structure of the PSD function is consistent with experience, however, for some body geometries and flow conditions the DeChant and Smith model requires additional verification to be of value as pertaining to the supporting quantities:

1. Critical/dominant fluctuation frequency
2. Loading amplification near the dominant frequency due to damping in current formulation
3. Root- mean square (RMS)/PSD magnitude.

We start by describing the basic DeChant/Smith PSD model paying particular attention to the role of the critical frequency and the amplification of the PSD at this frequency. Physics-based critical frequency model estimates are examined and compared to both high fidelity simulation results and experimental measurements. Finally, the PSD magnitude closure is examined in detail. The net result of this discussion is to examine the essential components of the PSD model in light of physics-based processes.

## II. Analytical Models: Development and Comparison to Representative Data Sets

Here we start by examining the base pressure fluctuation model [1].

### (1) Base Pressure Fluctuation: DeChant-Smith (2011)

Base pressure fluctuations are approximately described by a simple model developed in [1]. The major result of the model is an estimate for the base pressure fluctuation is the base pressure fluctuation PSD (i.e. ASD). The result is a spatial average across the base of the body and is thereby not spatially dependent. Similarly, spatial coherence information plays no role in this formulation.

Following [1], we describe this model as:

$$\Phi_{pp}(\omega) = \Phi_{mag} \frac{\left(a^2 + c^2 + \omega^2\right)}{\left(a^2 + c^2 - 2a\omega + \omega^2\right)\left(a^2 + c^2 + 2a\omega + \omega^2\right)} \tag{1}$$

Where we define the expressions:

$$a = \left(\frac{1.53 S_t (1 + C_D)}{2\pi^2 C_D}\right)^{1/2}$$

$$\Phi_{mag} = \frac{D}{U} \frac{(1.75(2)(K_C) a q_e)^2}{(1 + M_e)^4}$$

This formulation is described in detail in [1], but we include a typical result in Figure 2 which compares low speed measurements to the associated theory.

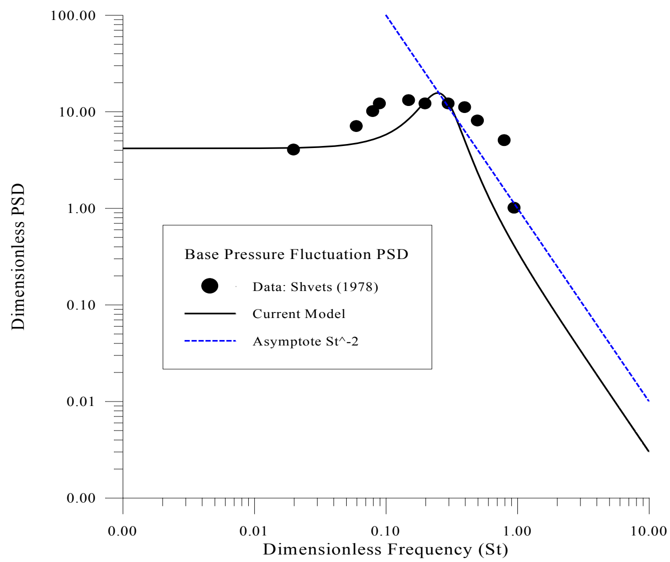


Figure 2. Typical base pressure PSD result emphasizing the relative importance of the critical frequency location at the maximum of the PSD magnitude.

We emphasize that the maximum PSD magnitude is associated with the critical frequency that is denoted by the Strouhal number. The Strouhal number can be empirically estimated by the expression: $St = \dfrac{\frac{1}{2\pi^2}K\left(1+C_D\right)}{C_D + \frac{4NK}{\mathrm{Re}}}$

where the empirical constants are K=1.53 and $\mathrm{Re} = 4NK$.

While we have access to the critical Strouhal number via this semi-empirical closure, there is obvious value in understanding the "provenance" and limitations of this type of result by examining the physics of this problem by surveying and developing Strouhal number models. Further, the PSD magnitude increase associated with the critical frequency is largely driven by the magnitude of the damping term in "c" in equation (1), implying that justification for the estimated value described previously is necessary. Finally, the magnitude behavior of the PSD needs to be understood, especially, for compressible high-speed flow regimes.

**(2) Critical Strouhal Number**

To get a general sense of the efficacy of the previous (critical) vortex shedding Strouhal number models, let's examine several typical problems. Perhaps the simplest result is to estimate the cone vortex shedding frequency using the aforementioned Ahlborn model: [2] $St = \dfrac{\frac{1}{2\pi^2}K\left(1+C_D\right)}{C_D + \frac{4NK}{\mathrm{Re}}} \approx \dfrac{\frac{1}{2\pi^2}K\left(1+C_D\right)}{C_D}$ which can be approximated by: $St \approx \dfrac{\frac{1}{2\pi^2}K\left(1+C_D\right)}{C_D}$ for large Reynolds numbers. Obviously, a key feature of this result is to estimate the associated drag coefficient since it represents the main connection between flow geometry and associated shedding frequency. The physics of this connection to the drag is perhaps not particularly clear, but a discussion described in Appendix I connects classical low speed concepts to the current approach. To apply, the current model to estimate the Strouhal number, we examine drag for conical bodies.

Drag coefficients for cones and cylindrical after bodies may vary considerably, but measurements [4] provide estimates that suggest: cone drag can be on the order of $C_d$=0.9. We warn, however, that this value is large for a drag coefficient, which may be attributable to the rarefied conditions for these measurements.

We can plot the Strouhal number as a function of the drag coefficient as depicted in Figure 3. As indicated, we note that hypersonic cone drag estimates tend to suggest that drag coefficients may be much smaller than described previous with $C_D$=0.1-0.2. This smaller value is in accord with the very simple expression for cone drag: $C_D = 0.0112\theta_{c\_\deg} + 0.162$ [5] suggesting that we could write:

- $C_D(\theta_{c\_\deg} = 5) = 0.22 \rightarrow St = 0.43$
- $C_D(\theta_{c\_\deg} = 10) = 0.27 \rightarrow St = 0.36$

Notice that these Strouhal numbers are seemingly large as compared to a more common result with St≈0.25 that was described in [1].

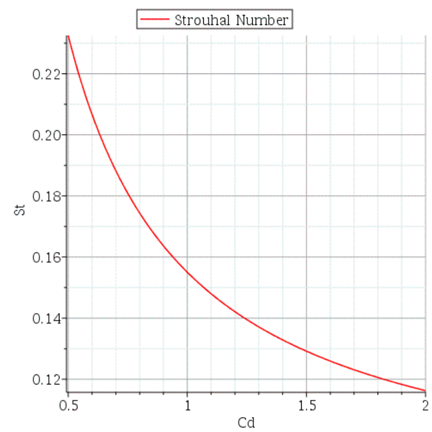


Figure 3. Strouhal number as function of body drag via Ahlborn model [2]. Notice that drag will need to be large for reasonable shedding frequencies.

We need to examine the efficacy of the Ahlborn [2] e.g., $St \approx \frac{\frac{1}{2\pi^2} K(1 + C_D)}{C_D}$. This model was developed for typically large blunt body problems at lower speeds. A model that is more appropriate for high-speed flow (based on Mach 14 experiments for cones 15 deg and spherical bodies) is described by [6]. The result of their effort is to derive an expression for the Strouhal number as:

$$St_\theta = \frac{f\theta}{U} = 0.229(1 - \frac{1820}{\mathrm{Re}_\theta}) \quad \theta = \left(\frac{C_D A}{2\pi}\right)^{1/2} \tag{2}$$

Now, more meaningfully, we can estimate that: $\frac{1820}{\mathrm{Re}_\theta} << 1$ so that we can write (for an axisymmetric base problem):

$$St_D = \frac{fD}{U} \approx \frac{\sqrt{2}}{4}(0.22)C_D^{-1/2} \tag{3}$$

Which plotted gives:

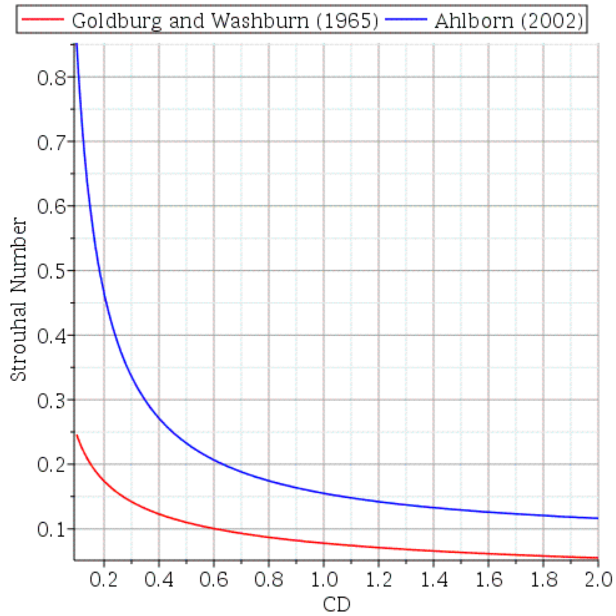


Figure 4. Comparison between Goldburg-Washburn [6] Strouhal number and Ahlborn model for Strouhal number. We propose that the Goldburg and Washbun [6] is likely more appropriate.

Using the [6]expression for our estimates of $C_D$

- $C_D(\theta_{c\_\deg} = 5) = 0.22 \rightarrow St = 0.16$
- $C_D = 0.9 \rightarrow St = 0.082$

Clearly, there is rather considerable variation associated with the appropriate drag coefficient for conical bodies. Estimates from measurements are, of course, useful. Krasilshchikov et. al. [7] estimates hypersonic drag coefficients (15 deg cone) on the order of $C_D$=0.2. Pick et. al. [8] suggests CD=0.1 for M=6 (10 deg) sharp cone.

**(a) High Fidelity Simulation versus Janssen and Dutton [9]; Kirchner et. al. [10]**

Let's then in turn examine measured afterbody pressure behavior as described in the literature with associated high-fidelity simulations. Consider the experiment by [9] who consider a Mach 2.46 flow past a 63.5 mm diameter cylinder. An estimate for dominant behavior is St=0.094. Flow conditions yield U=569 m/s implying that: $f = St\frac{U}{D} = \frac{569}{0.0635}(0.094) = 842Hz$. Examination of the simulation data (**pre-multiplied spectra f*PSD**) suggest that f=1000Hz signifying that the pre-multiplied spectra bias the peak estimate. Note that measurements [11] provide estimates for base pressure fluctuation for a blunt body. Their results indicate that the Strouhal number can readily be less than 0.1.

The base pressure Strouhal models need access to drag coefficient $C_D$; let's examine estimates for the Janssen and Dutton experiment. We have relatively little information for this problem in terms of the total drag since we do not readily have information for the upstream body. For some problems, the drag coefficient is dominated by the base drag (low pressure zone in the body base region). Obviously, a significant part of our effort has been to estimate the base pressure behavior for hypersonic bodies. Fortunately, the base pressure ratio described by equation (2) is directly related to the base pressure ratio via the base pressure coefficient as: $C_{D\_base} = -C_{p\_base}$. This, can in turn, be related to the base pressure ratio $\frac{p_b}{p_\infty}$ using:

$$C_{D\_base} = 2\left(1-\frac{p_b}{p_\infty}\right)\left(\frac{q_\infty}{p_\infty}\right)^{-1} = \frac{2}{\gamma M_\infty^2}\left(1-\frac{p_b}{p_\infty}\right) \quad (4)$$

Using reasonable estimates for the Reynolds number (Unit Reynolds number is 5E7/m) as with Res=2E6 and modeling the problem as 5-degree cone ( $M_e \approx M_\infty$). The result is presented below where the single measurement follows from a similar supersonic wake simulated using high fidelity methods (LES) i.e. Kirchner and Dutton [9]. Theory-based estimates are possible (see Appendix II) for the base pressure ratio and are presented in Figure 5.

We can use equation (4) to then estimate the base drag for this experiment as: $C_{D\_base} = \frac{2}{\gamma(2.46)^2}(1-(0.5)) = 0.12$. Corresponding Strouhal numbers for this value are 0.72 and 0.22, [2], respectively. Obviously, these values are probably much too large; suggesting that the drag coefficient is too small since a larger value for the base drag will imply a smaller value for the Strouhal number and better agreement with the data sets.

The largest plausible (possible) drag coefficient is $C_d = O(2)$ implying that St=0.115 using the Ahlborn approach. The Goldburg values would imply St=0.055. However, this value is usually for a 2-d shape e.g., elongate bar and would be seemingly much too large. A more useful estimate would be for an elongated cylinder aligned with the flow, as discussed by [12]. Notice, however, if we use the Goldburg et. al. model for $C_D$=0.4-0.5, [12] we would yield St=0.078-0.12 whereby: $f = St\frac{U}{D} = \frac{569}{0.0635}(0.078-0.12) = 985-1075Hz$, seemingly bounding the base pressure frequency.

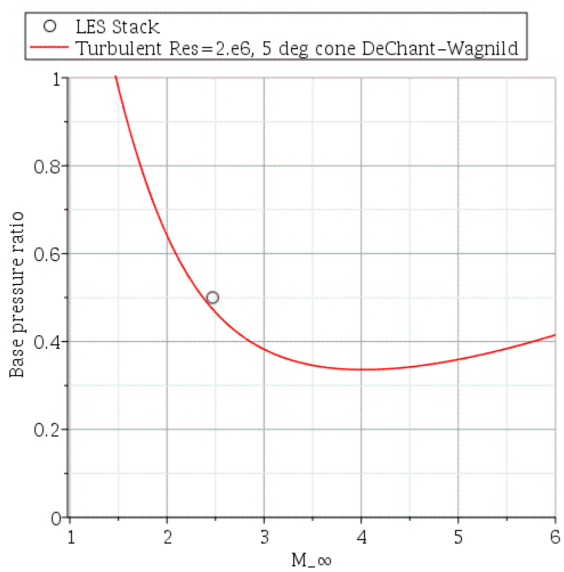

Figure 5. Comparison between base pressure model and LES simulation for [9],[10] base flow problem.

High fidelity simulations (LES) have been performed for a similar problem [10]. A typical PSD result is shown for the centerline value as St=0.09. Application of this value gives: $f = St\frac{U}{D} = \frac{569}{0.0635}(0.09) = 806Hz$, which is in excellent agreement with measurement.

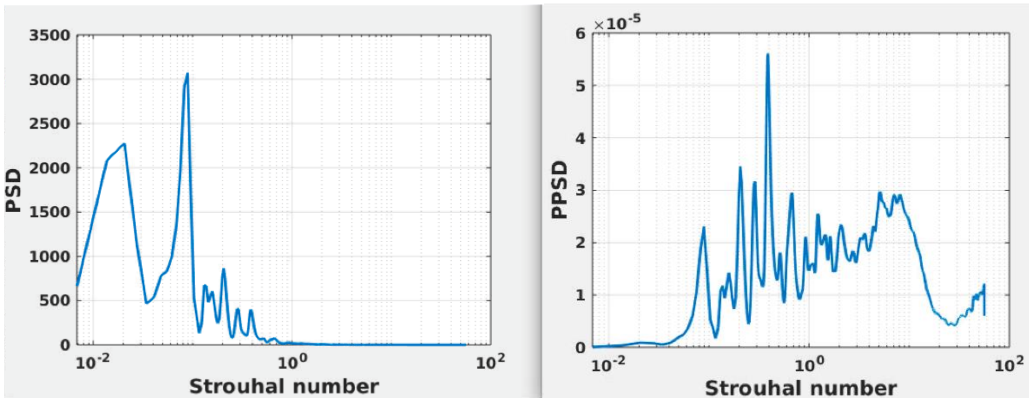


(a) PSD (b) pre-multiplied PSD

Figure 6. Base pressure fluctuation model for Kirchner Dutton [10] experiment. Notice the shift in the peak frequency between the two approaches.

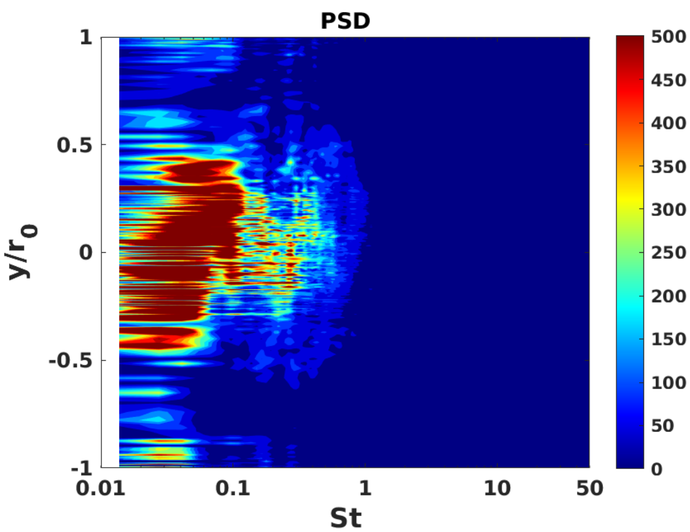


Figure 7. Pressure fluctuation over base of cylindrical body; Kirchner and Dutton [10]).

The PPSD is often utilized such that equal area under the PPSD function are correlated with equal power ($p'^2$). Nonetheless, notice as well, the frequency shift between the PSD and PPSD or pre-multiplied PSD.

**(b) Offset Sting Cone M=8 Measurements with Limited Bladed Mounted Cone Results**

Dedicated (Sandia) experimental results have been performed to support the flow behavior associated with high-speed conical base flow problems [13]. Examination of the current measurements yields U is on the order of U=1160 m/s while the base diameter is 0.0762 m. The flow is a high-speed Mach 8 condition. Measurements suggest that there is a lower frequency peak associated with this flow at approximately 700 Hz. This frequency implies that the Strouhal number should be on the order of $St = \frac{fD}{U} = \frac{(700)(0.077)}{1160} = 0.046$. This is a smaller Strouhal number than we might expect for the cone problem and via the expression: $St_D = \frac{fD}{U} \approx \frac{\sqrt{2}}{4}(0.22)C_D^{-1/2}$ requires a large value for cone drag coefficient. Indeed, using the current model for Strouhal number would have required a value for $C_D$=2.9 which is impossibly large. If we used a drag value of say 0.2 in the [6] expressions

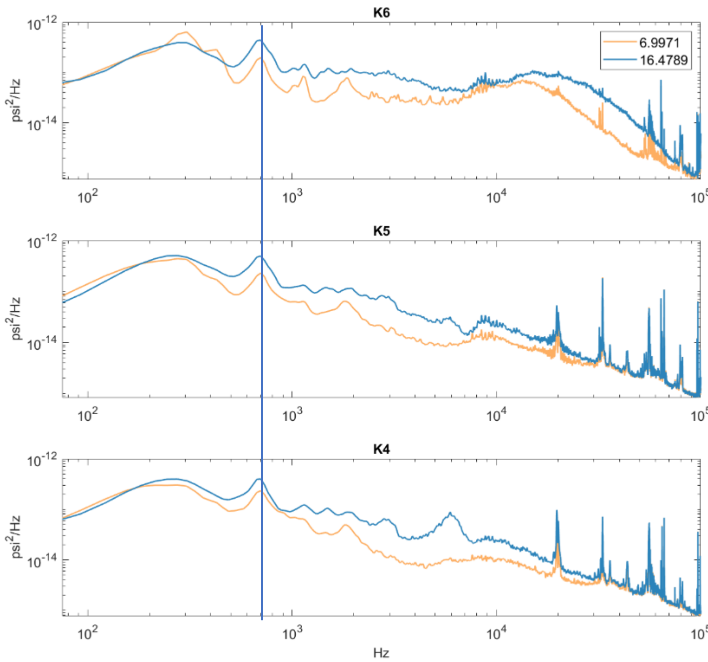


Figure 8. HWT Mach 8 offset sting pre-multiplied spectrum [13] for 5 deg cone; suggesting a peak at 700Hz.

While our analysis does not seem capable of estimating sufficiently low frequency (small Strouhal number) behavior, small values are known. Indeed, [3] mentions that the frequency of base shedding decreases with Mach number. He provides a graph which demonstrates this behavior. Notice for that for low supersonic Mach number, increasing Mach number implies reduction in Strouhal number. However, this reduction is limited for high Mach number. While useful, we need to be careful since this expression is likely associated with the premulitiplied frequency.

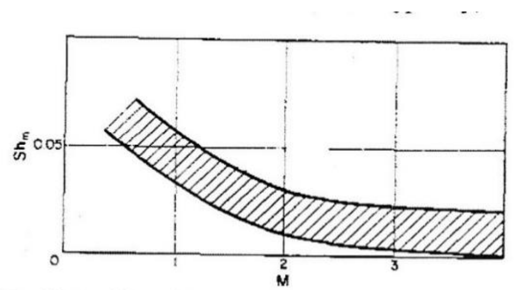


FIG. 23. Position of the maximum in the spectrum of the base pressure fluctuations for a cylinder with a conical nose ($D = 60$ mm, $L = 250$ mm).

Figure 9. Reduction in peak frequency as a function of Mach number; following [3].

An experimental and computational study that exhibits low frequency peaks is described by Saile et. al. [14]. Their study for a blunt coned cylindrical body with an axisymmetric extension in the base (not a sting mount, but a nozzle model) suggest that the relatively large diameter (40% of the diameter) impacts the associate base spectra by lowering the Strouhal number to be on the order of 0.025-0.03

#### (c) Shear Layer Fluctuation Behavior

Lower frequency behavior in the wake zone can be difficult to reconcile with the vortex shedding behavior described previously. There are, however, lower frequency unsteady behaviors that are associated with the Kelvin-Helmholtz behavior associated with the wake/recirculation shear zone behavior. Let's examine these results using some simple theoretical estimates for the behavior. The Kelvin-Helmholtz instability is very well known, and we can use some of the classical (inviscid) theory to help us estimate the frequencies associated with the most critical (fastest growing) disturbance. Briefly, the governing equations [15] associated with inviscid flow (Rayleigh equation) are simply:

$$\frac{d^2 f}{dy^2} - k^2 f - \frac{\frac{d^2 u}{dy^2}}{u - \frac{\omega}{k}} = 0 \tag{5}$$

Where f is related to the stream function (2-d) as: $\psi = f(y)\exp(i(kx - \omega t))$. Solution of equation (8) is challenging, but simplifies considerably if we describe the u(y) with piecewise linear profile with appropriate boundary condition connecting them $f(L^+)=f(L^-)$ and $(u-\omega/k)f'(L)=f(L)du/dy$. Notice that $\frac{d^2 u}{dy^2} = 0$. Consider now the linear profile given by:

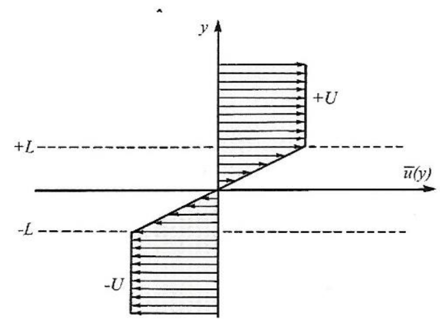


Figure 10. Piecewise linear profile representing wake/recirculation bubble interface [15].

Using the previous expressions, we can compute an expression for $\left(\frac{\omega}{k}\right)^2 = 0$ as:

$$\omega^2 = \frac{1}{4}\left(\frac{U}{L}\right)^2 \left((1-2kL)^2 - \exp(-4kL)\right) \tag{6}$$

The fastest growing (most dangerous) growth rate/frequency i.e., ω is computed via the derivative to give: $kL = 0.398 \approx 0.4$ whereby $\omega = 0.20\left(\frac{U}{L}\right)$. To utilize this result, we need to make estimates for value of L. A perhaps reasonable approach to estimate the shear layer width would be to delineate $L=R/2=D/4$ with $U_\infty/2<U<U_\infty$, Recognition that $k = \frac{2\pi}{\lambda} \rightarrow \lambda = \frac{2\pi}{0.4L}$ then gives:

$$f = \frac{\frac{\omega}{k}}{\lambda} = \frac{\omega}{2\pi} = \frac{(0.20)(0.40)}{2\pi}\left(\frac{U}{L}\right) = 0.051\left(\frac{U}{D}\right) \tag{7}$$

This expression suggests that low frequency/small Strouhal number behavior may indeed be possible for base flow behavior. Here, we emphasize, that this low frequency behavior is not associated with the vortex shedding behavior but is contained within the shear layer model.

### (3) Loading Amplification Near the Dominant Frequency Due to Damping

As describe by equation (1), [1] derived expressions for the base pressure fluctuation and proposed a PSD of the form:

$$\Phi \propto \int_0^\infty \cos(\alpha x)\exp(-\beta x)\cos(\omega x)dx = \frac{\alpha^2+\beta^2+\omega^2}{(\beta^2+(\alpha+\omega)^2)(\beta^2+(\alpha-\omega)^2)} \quad (8)$$

Where α and β are parameters, α being the critical dimensionless wave number/Strouhal number described previously. We have intentionally introduced a different notation to emphasize the general nature of the closure approach. The damping term β (equivalent to "c" in equation (2) was estimated using some physical arguments previously but is rather less well described and needs to be estimated for the local shear problem. Fortunately, classical turbulent shear behavior is well-known in the literature and can be used to estimate pressure fluctuation statistics.

Consider, the classical solution for a 2-d mixing layer with the mean flow behavior [16] written as:

$$u(x,y) = U_1 + \frac{1}{2}(U_2-U_1)(1+erf(\sigma\frac{y}{x})) \quad (9)$$

Where the constant σ is a dimensional constant that is $O$(1-10) depending on our definition approach.

The most important associated result follows that we can write the Reynolds stress in the form $u'v' \propto (U_2-U_1)x\frac{\partial u}{\partial y} = (U_2-U_1)^2\exp(-(\sigma\frac{y}{x})^2)$ or grossly approximating a pressure fluctuation magnitude: $p' \sim \rho u'u' \propto \rho(U_2-U_1)^2\exp(-(\sigma\frac{y}{x})^2)$. Notice that we are using a simple ansatz relating pressure fluctuation to velocity fluctuation $p' \sim \rho u'u'$ that is common for isotropic turbulence [16].

Considering y>0 only we can approximate: $p' \sim \exp(-2\sigma\frac{y}{x})$ and then compute an estimate for the later correlation $R_y$(dy) as:

$$R_y(\Delta y) = \int_0^\infty \exp(-2\sigma y)\exp(-2\sigma(y+\Delta y)) \propto \exp(-2\sigma\Delta y) \quad (10)$$

Access to the cross-stream correlation then implies that we can pose the correlation-coherence constraint as:

$$R_y(y) = \exp(-2\sigma y) = \int_0^\infty \Phi(\omega)\exp(-B\omega y)d\omega \quad (11)$$

Where, of course, $\Phi \propto \dfrac{(\alpha^2+\beta^2)(\alpha^2+\beta^2+\omega^2)}{(\beta^2+(\alpha+\omega)^2)(\beta^2+(\alpha-\omega)^2)}$ , $\exp(-B\omega y)$ is the lateral coherence across the base of the bluff body and C is a scaling constant.

Unfortunately, the resulting integral $\int_0^\infty \Phi(\omega)\exp(-B\omega y)d\omega$ is very complex and yields results that are not amenable for further analysis. A simple functional analysis approximate is appropriate here. Consider the closure (integral constraint) $\Phi \propto \exp(-\gamma\omega)$ where:

$$\int_0^\infty \exp(-\gamma\omega)d\omega = \int_0^\infty \frac{(\alpha^2+\beta^2)(\alpha^2+\beta^2+\omega^2)}{(\beta^2+(\alpha+\omega)^2)(\beta^2+(\alpha-\omega)^2)}d\omega \tag{12}$$

To give $\gamma = \dfrac{2}{\pi}\dfrac{\beta}{(\alpha^2+\beta^2)}$.

We are now able to write the coherence constraint as:

$$f(y,\alpha,\beta,B,C) = \exp(-2\sigma y) - C\int_0^\infty \exp(-\frac{2}{\pi}\frac{\beta}{(\alpha^2+\beta^2)}\omega)\exp(-B\omega y)d\omega = 0 \tag{13}$$

which is a residual expression with several unknown parameters e.g., β, B and C (α is known) valid for $0<y<\infty$.

We can compute estimates for the unknown parameters by demanding satisfaction of the residual. For example, by evaluating f(y=0) the resulting algebraic expression gives:

$$f(0,\alpha,\beta,B,C) = 0 \rightarrow C = \frac{2}{\pi}\frac{\beta}{(\alpha^2+\beta^2)} \tag{14}$$

Of greater interest, however, is an estimate for β. We compute this value by using the derivative constraint:

$$f'(0,\alpha,\beta,B,C = \frac{2}{\pi}\frac{\beta}{(\alpha^2+\beta^2)}) = 0 \rightarrow \beta = \frac{2\sigma - \sqrt{4\sigma^2 - \pi^2\alpha^2B^2}}{\pi B} \tag{15}$$

Finally, we can estimate, the coherence constant B as:

$$f''(0,\alpha,\beta,B = \frac{2\sigma - \sqrt{4\sigma^2 - \pi^2\alpha^2B^2}}{\pi B}, C = \frac{2}{\pi}\frac{\beta}{(\alpha^2+\beta^2)}) = 0 \rightarrow B = \sqrt{2} \tag{16}$$

Thus, we can obtain estimates for parameters in preceding equations

We are most interested in the damping β since it is this term that dramatically influences the behavior of the PSD. As such, we can consider in more detail the size of this term. Let's then consider the expression for β

$$\beta = \frac{2\sigma - \sqrt{4\sigma^2 - \pi^2 \alpha^2 B^2}}{\pi B} \approx \frac{\sqrt{2}\pi}{4} \frac{\alpha^2}{\sigma} \tag{17}$$

Thus, we can see that for small α that the damping term will be small. Moreover, the PSD $\Phi \propto \frac{(\alpha^2+\beta^2)(\alpha^2+\beta^2+\omega^2)}{(\beta^2+(\alpha+\omega)^2)(\beta^2+(\alpha-\omega)^2)}$ is then no longer a function of two variables but is a function of the critical frequency α only. Indeed, using this closure and with σ=1 we can plot the scaled PSD as:

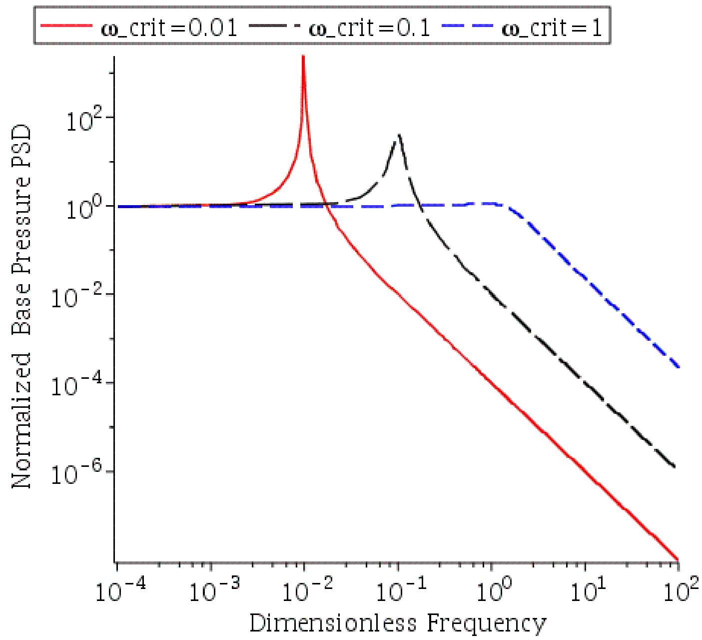


Figure 11. Base pressure PSD for several critical frequencies demonstrating the increase in magnitude near the critical frequency.

Let's examine more completely the results expressed here by considering the implications of the damping term identified in equation (17) as it provides an estimate for the damping behavior. To use equation (17) we will need an estimate for the turbulent spreading rate term σ. Traditionally, for a mixing layer, σ=13.5 [16], and smaller values are used for jets i.e., σ=7.7. However, compressible mixing is typically significantly suppressed as compared to incompressible behavior. Moreover, the use of the mixing layer formulation is only an analogy for wake flow. Indeed, the 2-D mixing layer expressed by equation (9) can be modified to provide a defect velocity formulation as:

$$u(x,y) = 1 - erf(\sigma_{eff}\xi)) \tag{18}$$

Which can be more readily compared to the wake defect velocity as:

$$u(x,y) = \exp(-\frac{1}{2}\sigma_{wake}\xi^2)) \tag{19}$$

Knowing the value for $\sigma_{wake}$ we can estimate an effective mixing layer result by using an elementary functional approximation (integral constraint) as:

$$\int_0^\infty 1 - erf(\sigma_{eff}\xi))d\xi = \int_0^\infty \exp(-\frac{1}{2}\sigma_{wake}\xi^2))d\xi \rightarrow \sigma_{eff} = \frac{(2\sigma_{wake})^{1/2}}{\pi} \quad (20)$$

Using a wake value $\sigma_{wake} \approx 10 \rightarrow \sigma_{eff} = 1.4$; implying that an estimated value in the preceding analysis should be $O(1)$.

Using this estimate for σ we can utilize equation (23) to estimate damping β as a function of the dimensionless frequency α as:

$$\beta = \frac{\sqrt{2}\pi}{4}\frac{\alpha^2}{1.4} \quad (21)$$

Implying that the damping parameter is directly related to the critical frequency. *How well does this approximation agree with previous modeling efforts?* In reference [1], a typical value for the critical frequency (Strouhal number) was estimated as (using current notation): α=0.257. This value implies (through equation (21)) that $\beta = \frac{\sqrt{2}\pi}{4}\frac{(0.257)^2}{1.4} \approx 0.052$. This value is in excellent agreement with the damping constant recommended for use with $\beta = \frac{1}{20} = 0.05$. We emphasize, that while this agreement is very good, that the analyses used to create are quite approximate and the result should be only used as a guide. Nonetheless, the closure for the damping term derived here provides a useful support to the previously developed PSD model.

**(4) RMS Pressure Fluctuation Values**

An estimate for the magnitude associated with pressure fluctuation and inherently connected to the PSD/ASD magnitude is the Root Mean Square RMS values, i.e., $p_{rms}$. The importance of this quantity in describing the magnitude of the fluctuations means that several empirical and semi-empirical estimates are available. The most classical result is that by Shvets [3] who describe the empirical expression:

$$\frac{p_{rms}}{q_\infty} = \frac{0.06}{(1 + M_\infty)^2} \quad (22)$$

In their monograph Chaump, et. al. [17] examine high Mach number sharp cone behavior. Their model follows as:

$$\frac{p_{rms}}{p_b} = \frac{0.01M_b^2}{1 + 0.04M_b^2} \quad (23)$$

Where here, $p_b$ is the base pressure and $M_b$ is the somewhat ill-defined base Mach number. Obviously, the base pressure can be related to the base pressure ratio $\frac{p_b}{p_\infty}$ which in turn be related to the dynamic pressure. Further, for small half angle cones, the base pressure Mach number can be approximated equated to the free-stream value (local expansion, but viscous reduction):

$$\frac{p_{rms}}{q_\infty} = \left(\frac{2}{\gamma M_\infty^2}\right)\left(\frac{p_b}{p_\infty}\right)\frac{0.01M_\infty^2}{1 + 0.04M_\infty^2} \quad (24)$$

Further, we have access to experimental measurements for sting mounted base pressure measurements (5 deg cone Mach 5 and Mach 8) [13] as well as Mach 2.45 simulations. These values can be plotted to give the result in Figure 12. The implementation following [1] utilizes the Shvets [3] type Mach number behavior. We suggest that this model provides a useful intermediate result for a range of Mach numbers.

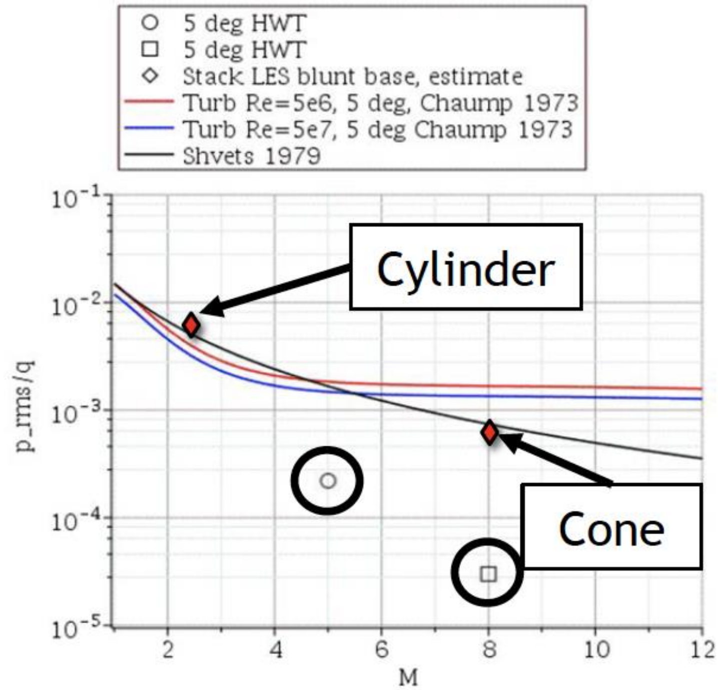


Figure 12. RMS pressure fluctuation for 5 deg sharp cone using the Shvets [3], Chaump et. al. [17] models compared to LES computation (Stack) and sting mounted HWT [13] measurements. The HWT measurements (highlighted by dark circles) seem to underestimate the RMS values.

There is value in examining the low values of the High-speed Wind Tunnel (HWT) RMS pressure fluctuation results [13] as compared to simulation and analytical expressions shown in Figure 12. We suggest that a possible bias towards reduced pressure fluctuation magnitude is associated with the wind tunnel model support i.e., the offset from center base mounted sting. While this potential bias was of concern, there was little direct evidence to support the degree of bias etc. Fortunately, a subsequent set of tests led by Saltzman have been completed using an alternative blade mount that does not introduce local base blockage. Moreover, a broad suite of additional computations that examined the role of base mounting were performed. Comparison of these results for a HWT configuration (symbols) plotted with the simulation results (lines) clearly suggest that the sting mount causes a significant reduction in the local pressure fluctuation magnitude, implying that the sting mount interference limits the viability of these measurement in the base flow region.

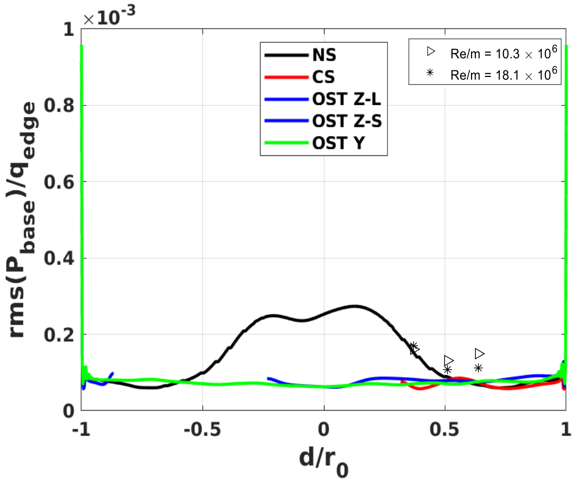


Figure 13. RMS pressure fluctuation measurements for 5-degree sharp cone using blade mounted sting (symbols) versus simulation (NS: No Sting, CS: Center mounted Sting, OST etc: Offset Sting are various offset sting location) for Mach 8 demonstrating that the measurements are in good agreement with the No Sting case. These measurements and simulations results suggest that the presence of the base sting likely biased the previous RMS measurements.

In summary, the development described here has focused on examining several key components of the DeChant-Smith base pressure fluctuation PSD model. Here our goal has been to examine these features as pertains to physical basis and high speed/compressible effects. Examination of available information from the literature, dedicated high fidelity simulations and in-house supporting experimental measurements. These results suggest that the current approach is likely an adequate model for sphere-cone geometries for a range of flow conditions.

# III. Conclusion

The preceding development demonstrate that the current employed PSD models provides a viable reduced order closures for turbulent base pressure fluctuations for high Reynolds number flows over range of Mach numbers. Access to a reliable base pressure fluctuation reduced order model as described by [1] then permits simulation of bluff body vibratory input as required for fluid structure interaction problems. We have specifically focused on:

1. Critical/dominant fluctuation frequency
2. Loading amplification near the dominant frequency due to damping in current formulation
3. Root- mean square (RMS)/PSD magnitude.

Confidence in the adequacy of this approach was established using a detailed high-fidelity computational study is compared to measurements by Janssen and Dutton [9], dedicated Mach 8 cone base measurements for several model mounting configurations [13] with attendant high-fidelity simulations showing support for theory-based closures, and several theory-based approaches that strongly support the original PSD model behavior. The role of high-fidelity Large Eddy Simulation (LES) and measurement has been highlighted. Mounting configuration for wind tunnel test has been shown to be important for base pressure measurement with the minimal blockage blade mounted support providing minimal base interference. This study also serves to illustrate the supportive interaction between approximate theory, high-fidelity simulation, and wind tunnel measurements in characterization of a complex physical phenomena.

# IV. Appendix I: Classical Derivation for Bluff Body Shedding Frequency

Base pressure fluctuation behavior in the lee of a blunt body is characterized by large scale unsteady behavior, a situation consistent with the classical von Karman vortex street. Though the turbulent wake of high Reynolds number problems does not exhibit the classical periodic street, as noted by Rigas [18] “Despite their turbulence, such wake flows exhibit organization which is manifested as coherent flow structures; these are usually associated with increased noise, structural fatigue and drag." Thus, characterization of large-scale frequency behavior for bluff body flow becomes essential.

The previous analysis developed by [1] yielded estimates for the base pressure fluctuation PSD. Within that analysis is the critical estimate for the dimensionless frequency (Strouhal number) of the coherent structures. The development by [1] followed [2]to give the Strouhal number the result:

$$S = \frac{\frac{1}{2\pi^2} K(1+C_D)}{C_D + \frac{NK}{\mathrm{Re}}} \tag{A.1.1}$$

A typical estimate for S envisions Re>>1 and $K \approx 1.53$. Using these values, a high Reynolds number estimate for a <u>normal plate</u> would be: $C_D$=1.7 and S=0.21 (measurements from [19] suggest S=0.135).

The preceding estimates for the shedding frequency suggest that there may be value in reviewing the Strouhal number estimates used in the base pressure fluctuation model. A perhaps natural place to start this process is to examine the classical approach developed by [19] and others. The Roshko [19] approach is one based upon a classical model for a von Karman vortex street represented by two series of point vortices of equal strength separated by periodic distance "a". Each modeled vortex is separated from the other by distance "b". This simple model is described by Goldstein [20]. While relatively simple in form, this model a significant degree of information. Using this model, we can estimate the drag on the bluff body as:

$$C_D = \frac{h}{d}\left(5.56\frac{u}{U} - 2.25\left(\frac{u}{U}\right)^2\right) \tag{A.1.2}$$

Where h is the width of the wake and is set equal to the shear layer spacing with h=b and u is the speed associated with the vortex sheet relative to the free stream U. The strength of the vortices is directly related to the shear layers. Roshko [19] uses this information to provide a connection between the base pressure parameter "k" (which is directly related to the increased velocity needed to negotiate the blockage of the body as: $k = \frac{u_s}{U} > 1$. The relationship derived by Roshko states that:

$$\frac{u}{U} = \frac{1}{2}\left(1 + \sqrt{1 - \frac{\sqrt{2}}{2}ck^2}\right) \tag{A.1.3}$$

Notice here the introduction of a term "c" which is related to the amount of vorticity generated by the bluff body compared to the amount that is captured in the vortex street. Traditionally we estimate that about 50% of the generated vorticity is captured in the vortex system. We will propose that c is closer to 0.4-0.45 and is dependent on the type of bluff body. Unfortunately, the vortex frequency S will be shown to be sensitive to this parameter. We note that a very simple extension to our analysis involves correlating c with drag since separated flow bodies have a larger value for c as compared to less well-defined separation bodies (e.g., cylinder). An expression such as: $c = (0.45 - 0.4)C_D + 0.4$ will provide a useable approximation for c.

To complete the solution, we need to relate u/U to the vortex system spacing parameters. This is accomplished by referring to the analysis of Bearman [22] (who references the Kronauer stability criterion) which implies that the vortex system will conform to reach a state of minimum drag giving:

$$2\cosh(\pi\frac{b}{a}) = \left(\frac{U}{u} - 2\right)\sinh(\pi\frac{b}{a})\left(\cosh(\pi\frac{b}{a})\sinh(\pi\frac{b}{a}) - \pi\frac{b}{a}\right) \quad \text{(A.1.4)}$$

Equation (A.1.4) provides a mapping between b/a and u/U. The final expression necessary is to relate the drag back to the k e.g., $u_s$/U. While we normally think of drag as being based upon geometry only, a key generalization espoused by Roshko [1] was to include k information. Roshko [1] achieves this by solving a series of complex "notched hodograph" free-streamline problems. A more workable approach is simply to relate drag to k using parameterizations of these solutions. A workable expression is simply:

$$C_D = C_{D0}\left(\frac{k}{k_0}\right)^2 \quad \text{(A.1.5)}$$

Where $C_{D0}$ is the typical drag coefficient and $k_0$=1.5. An example of this model prescription is for a normal plate where $C_{D0}$=2. These expressions provide sufficient information to estimate the associates Strouhal number as:

$$S = \frac{fd}{U} = \frac{(U-u)}{a}\frac{d}{U} = (1-\frac{u}{U})\left(\frac{d}{h}\right)\left(\frac{b}{a}\right) \quad \text{(A.1.6)}$$

The preceding expressions, i.e. equations (A.1.2)-(A.1.6) provide sufficient information to estimate the Strouhal number S as a function of $C_D$ and $C_{D0}$. Unfortunately, the algebraic complexity of the associated expressions will make a closed form expression unavailable requiring us to exam typical cases. Let's consider several relevant cases:

| Bluff Body | $C_D$ | $C_{D0}$ | S (meas) | S (current) | Rel. Err. | S (Ahlborn) | Rel. Err. |
|---|---|---|---|---|---|---|---|
| 2-d cyl. | 1 | 1.1 | 0.21 | 0.23 | 10% | 0.15 | 30% |
| 2-d wedge | 1.3 | 1.3 | 0.18 | 0.22 | 30% | 0.14 | 22% |
| 2-d norm plate | 1.7 | 2.0 | 0.14 | 0.14 | 0% | 0.12 | 60% |
| sphere | 0.5 | 0.5 | 0.39 | 0.48 | 24% | 0.23 | 40% |
| cone (35 deg) | 0.6 | 0.6 | 0.45 | 0.41 | 9% | 0.21 | 48% |

Table A.1.1 Comparison between Strouhal number estimates as derived using the current (Roshko approach [19]) and the Ahlborn model [2]

The preceding analysis suggests that shedding frequency as computed using the current approach is likely an improvement over the empirically based Ahlborn model [2].

## V. Appendix II: Approximate Model for Mean Base Pressure

As noted in the text. estimates for the base pressure in the lee of hypersonic vehicles is an important quantity needed to provide estimates of the net drag force on the system. An extensive body of measurement, computation and theory-based literature is available to estimate base pressure, however, a very widely utilized family of empirical expressions proposed by Lamb and Oberkampf [21] have gained wide acceptance. Here, we consider a physics-based expression for the zero angle-of-attack base pressure derived using an approximate energy integral to connect the base expanded inviscid flow field to the mixing dividing streamline. The wake flow field is approximated using an elementary analytical approach. The mixing model is sensitized to compressibility using simple arguments. Finally, the dividing streamline pressure is projected onto the base via an isentropic argument. While the resulting analytical expression is simple, it appears to be capable of modeling base pressure Mach number and Reynolds number trends. The efficacy of the result is suggested by good comparison to the Lamb-Oberkampf correlation, as well as classical measurements. Since some of the Lamb-Oberkampf expressions can involve boundary layer edge pressure quantities which are not readily available within the scope of elementary correlations, approximate closed-form models are presented to relate these quantities back to more readily available information. The current approach provides useful insight into the near wake behavior for hypersonic bodies by providing approximate estimates for mean base pressure behavior.

Here we describe the turbulent version of the DeChant-Wagnild base pressure model. The derivation of these expressions is described elsewhere.

$$\frac{p_b}{p_\infty} = \left.\frac{p_b}{p_\infty}\right|_0 \left( 1 + \frac{\frac{\gamma-1}{2}(1-cM_e^{1.25})^2\left(\frac{u_D}{u_2}\right)^2 M_e^{2.5}}{1+\frac{\gamma-1}{2}[1-(1-cM_e^{1.25})^2\left(\frac{u_D}{u_2}\right)^2]M_e^{2.5}} \right)^{\gamma/(1-\gamma)} \tag{A.2.1}$$

Where,

$$\left.\frac{p_b}{p_\infty}\right|_0 = c_0\left(\frac{u_m}{u_2}\right)^2 = c_0\left(1-\frac{1}{2}\left(erf\left(\frac{\sqrt{2}}{4}\left(\frac{\mathrm{Re}_s}{\mathrm{Re}_{s0}}\right)^{1/2}\right)\right)\right)^2 \tag{A.2.2}$$

And the parameters are given by:
c = 0.025
$c_0$ = 5
$\mathrm{Re}_{s0}$ = 5E5
and

$$\frac{u_D}{u_2} = 1-\frac{1}{2}\left(erf\left(\frac{3\sqrt{2}}{16}\right)+erf\left(\frac{\sqrt{2}}{16}\right)\right) = 0.8$$

For a conical body, the edge Mach number is estimated using the Taylor Maccoll-based expression:

$$M_e^2 \approx \frac{M_\infty^2}{1+3\gamma M_\infty \sin^2\theta} \tag{A.2.4}$$

Where θ =cone half angle (radians). These expressions are utilized in the text to estimate the base pressure component of the net vehicle drag.

While the current effort is focused on base pressure fluctuation as opposed to mean base pressure the minimal base pressure interference offered by the blade mounted sting measurements offers an opportunity to compare the results of the mean base pressure models as described by equations (A.2.1) and (A.2.2) to experimental data. Figure (A.2.1) presents these results.

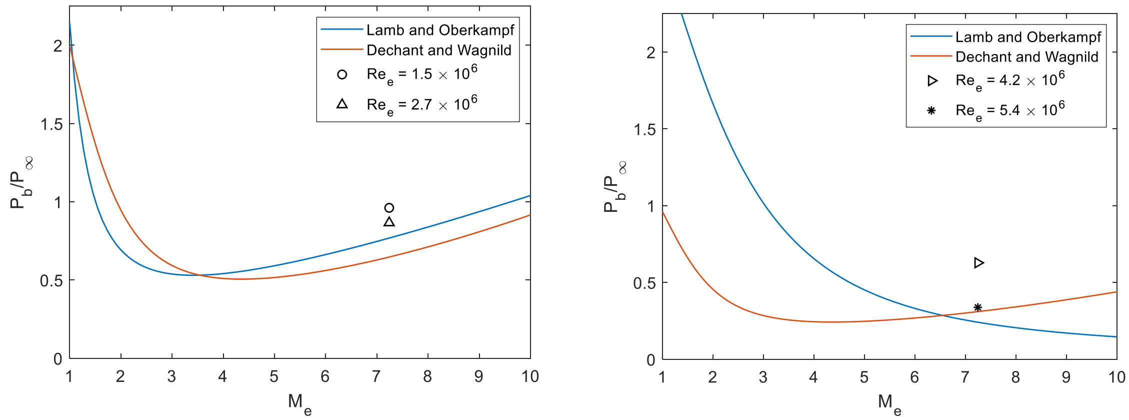


(a) Laminar (b) turbulent

Figure A.2.1: Comparison between empirical model e.g., Lamb and Oberkamf [21], current theory as equations (A.2.1) and (A.2.2) and blade mounted 5-degree cone, Mach=8 Saltzman HWT measurements suggesting reasonable agreement.

## VI. Acknowledgements

Sandia National Laboratories is a multi-mission laboratory managed and operated by National Technology and Engineering Solutions of Sandia, LLC., a wholly owned subsidiary of Honeywell International, Inc., for the U.S. Department of Energy's National Nuclear Security Administration under contract DE-NA0003525. We are grateful for the Sandia National Laboratory experimental measurement via offset sting by Yibin Zhang and the overall experimental program for sting and blade mount configurations by Katya Casper.

(1) DeChant, L. and Smith, J., An approximate expression for base pressure fluctuation spectra for bluff bodies, AIAA-2011-180.

(2) Ahlborn, B., Seto, M. L. and Noack, B.R. "On drag, Strouhal number and vortex street structure," *Fluid Dyn. Res.* **30**, 379 (2002).

(3) Shvets, A. I.; Base Pressure Fluctuations, Translated from *Zhurnal Prikladnoi Mekhaniki i Tekhnicheskoi Fiziki*, No. 2, pp. 65–72, March–April, (1973)

(4) Wendt, J. F., Drag Coefficient of Cones, VON KARMAN INST FOR FLUID DYNAMICS RHODE-SAINT-GENESE (BELGIUM), ADA 750042, 1972.

(5) Hoerner, S.F., Fluid-Dynamic Drag, /https://hoernerfluiddynamics.com/shop/, 1965.

(6) Goldburg, A., Washburn, W., Florsheim, B, Strouhal numbers for the hypersonic wakes of spheres and cones, AIAA Journal, 3,7, pp.1332-1333, 1965.

(7) Krasilshikov A P and Podobin V P 1968 Experimental research of free flight ball aerodynamic characteristics up to the Mach number 15. *Fluid Dynamics* **4** pp 190–193

(8) Pick, G. S., "Base pressure distribution of a cone at hypersonic speeds," AIAA J. 10, pp. 1683-1686, 1972.

(9) Janssen, J. R., & Dutton, J. C. (2004). Time-Series Analysis of Supersonic Base-Pressure Fluctuations. *AIAA journal*, *42*(3), 605-613.

(10) Kirchner B. M., Favale, J., V., Elliott, G. S., Dutton, J. C., "Three-component turbulence measurements and analysis of a supersonic, axisymmetric base flow," AIAA J. **57**, 2496–2512 (2019).

(11) Vikramaditya, N. S., Viji, M., Modes of Base Pressure Fluctuations: Shape, Nature, and Origin, AIAA JOURNAL, Vol. 57, No. 9, September 2019

(12) Prosser, D. T., Smith, M. J., Aerodynamics of Finite Cylinders in Quasi-Steady Flow, AIAA-2015-1931.

(13) Zhang, Y., Richardson, D., Beresh, S. J., Casper, K. M., Soehelle, M. M., Spiller, W. Hypersonic wake measurements behind a slender cone using FLEET velocimetry, AIAA Proceedings, AIAA Aviation 2019 Forum 17-21 June 2019 Dallas, Texas eISBN: 978-1-62410-589-0

(14) Saile, D., Gulhan, A., Henckel, A., Investigations on the Near-Wake Region of a Generic Space Launcher Geometry, AIAA-2011-2352.

(15) Drazin, P. G., Reid, W. H., Hydrodynamic Stability, Cambridge University Press; Online publication date: August 2010; Print 2004.

(16) Schlichting, H. (1968) Boundary-Layer Theory. 6th Edition, McGraw-Hill Book Company, New York
(17) Chaump, L. E.; Martellucci, A.; and Montfort, A.: Aeroacoustic Loads Associated with High Beta Re-Entry Vehicles. AFFDL-TR-72-138, Vol, lI, 1973.
(18) Rigas, G., Oxlade, A. R., Morgans, N . Morrison, J. F., Low-dimensional dynamics of a turbulent axisymmetric wake, J. Fluid Mech. (2014), vol. 755, R5, doi:10.1017/jfm.2014.449
(19) Roshko, A., On the Development of Turbulent Wakes from Vortex Streets, NACA, TR-11-91, 1954
(20) Goldstein, S., Modern developments in fluid dynamics, volumes I, II, Oxford Press, NY, 1956.
(21) Lamb, J. P., Oberkampf, W, L., "Review and development of base pressure base heating correlations in supersonic flow," *J. Spacecraft and Rockets*, 32, 1, 1995, pp. 8-23.
(22) Bearman, P. W., On vortex street wakes, JFM, 38, 4, pp. 655-641, 1967.